

## SUPPLEMENT OF THE ARTICLE

# Natural emissions of VOC and NO<sub>x</sub> over Africa constrained by TROPOMI HCHO and NO<sub>2</sub> data using the MAGRITTEv1.1 model

Beata Opacka<sup>1</sup>, Trissevgeni Stavrakou<sup>1</sup>, Jean-François Müller<sup>1</sup>, Isabelle De Smedt<sup>1</sup>, Jos van Geffen<sup>2</sup>, Eloise A. Marais<sup>3</sup>, Dylan B. Millet<sup>4</sup>, Kelly C. Wells<sup>4</sup>, Alex B. Guenther<sup>5</sup>

<sup>1</sup>Royal Belgian Institute for Space Aeronomy (BIRA-IASB), Brussels, 1180, Belgium

<sup>2</sup>Royal Netherlands Meteorological Institute (KNMI), De Bilt, the Netherlands

<sup>3</sup>Department of Geography, University College London, London, UK

<sup>4</sup>Department of Soil, Water, and Climate, University of Minnesota, St Paul, MN, USA

<sup>5</sup>Department of Earth System Science, University of California Irvine, 92697, California, USA

*Correspondence to:* Beata Opacka ([beata.opacka@aeronomie.be](mailto:beata.opacka@aeronomie.be)) and Trissevgeni Stavrakou ([jenny@aeronomie.be](mailto:jenny@aeronomie.be))

This supplement contains

1. Regional and temporal variability of a priori and optimised NO<sub>x</sub> and VOC sources (Fig. S1)
2. Top-down anthropogenic NO<sub>x</sub> and VOC (Fig. S2)
3. Comparison between in situ flux measurements and modelled fluxes (Table S1)
4. Uncertainties in TROPOMI-derived UT NO<sub>2</sub> (Fig. S3 and S4)
5. Optimised isoprene emissions (Fig. S5)

## 1. Regional and temporal variability of a priori and optimised NO<sub>x</sub> and VOC sources

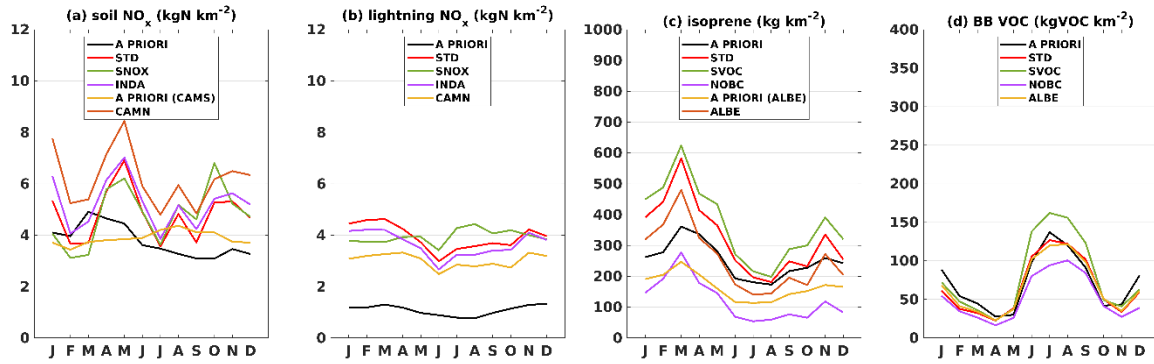
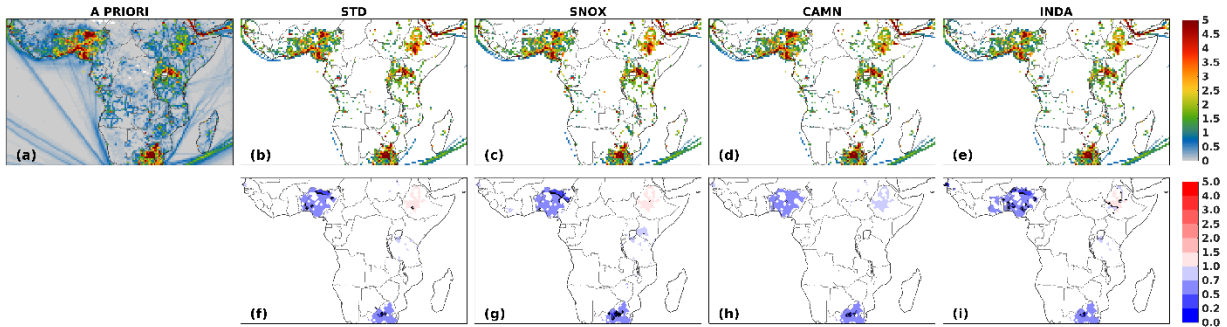


**Figure S1:** Seasonal variability of (a) soil NO<sub>x</sub> (in kgN per km<sup>2</sup>), (b) lightning NO<sub>x</sub> (in kgN per km<sup>2</sup>), (c) isoprene (in kg of isoprene per km<sup>2</sup>), and (d) biomass burning VOC (in kg VOC per km<sup>2</sup>) emissions for different inversions averaged over the entire continental domain.

## 2. Top-down anthropogenic NO<sub>x</sub> and VOC

(a) Anthropogenic NO<sub>x</sub>



(b) Anthropogenic VOC

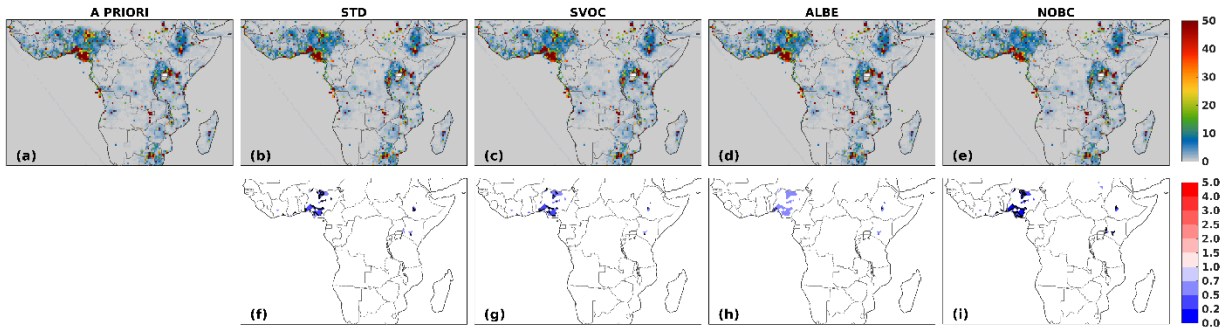


**Figure S2:** As in Fig. 11 and 13, but for anthropogenic (a) NO<sub>x</sub> and (b) VOC emissions, respectively. The fluxes are expressed in in 10<sup>10</sup> molec.cm<sup>-2</sup> s<sup>-1</sup> and the emissions increments are unitless.

### 3. Comparison between in situ flux measurements and modelled fluxes

**Table S1:** As Table 3, with additional model estimates at each site and corresponding months. Averages over all data, as well as data in dry and wet season are provided in the table.

	Location	Month	Season	OBS	A priori	STD	INDA	CAMN (a priori)	CAMN
1	Mayombe, Congo	6	W	1.74	1.62	2.32	2.40	1.57	1.78
		7	D	0.78	2.28	3.73	3.48	1.52	3.03
		2	W	0.50	0.51	0.74	1.15	0.87	1.61
2	Teke Plateau, Congo	4	W	0.03	0.77	0.95	1.30	1.15	1.31
3	Lamto, Ivory Coast	1	D	1.02	2.22	1.31	6.55	2.80	1.55
		5	W	0.74	1.24	0.64	1.57	1.60	0.81
4	Nylsvley, South Africa	3	W	2.98	0.67	0.61	0.60	1.30	1.96
5	KNP, South Africa	10	W	0.97	0.85	0.46	0.46	0.20	0.19
		11	W	2.13	0.92	0.66	0.65	0.26	0.35
		12	W	1.01	0.97	1.05	1.03	0.27	0.48
		8	D	3.17	0.34	0.40	0.39	0.17	0.33
6	Transvaal, South Africa	9	D	1.99	0.50	0.27	0.27	0.19	0.17
7	Marondera, Zimbabwe	10-12	W	4.85	2.58	4.10	4.04	1.61	3.90
8	Savè, Benin	6-7	W	2.06	0.74	0.29	0.55	1.81	0.58
9	Banizoumbou, Niger	8	W	2.62	0.66	0.49	2.29	2.34	1.85
10	Agoufou, Mali	7	W	2.88	3.51	3.54	4.16	1.43	2.91
		8	W	0.98	0.66	0.94	1.19	2.05	4.33
11	Dahra, Senegal	7	W	2.45	6.05	5.58	6.12	1.42	5.13
		11	D	1.72	4.57	2.58	4.26	1.39	1.43
<b>Average</b>				<b>1.82</b>	<b>1.67</b>	<b>1.61</b>	<b>2.23</b>	<b>1.26</b>	<b>1.77</b>
<b>Dry season average</b>				<b>1.74</b>	<b>1.98</b>	<b>1.66</b>	<b>2.99</b>	<b>1.21</b>	<b>1.30</b>
<b>Wet season average</b>				<b>1.85</b>	<b>1.55</b>	<b>1.60</b>	<b>1.97</b>	<b>1.28</b>	<b>1.94</b>

#### 4. Uncertainties in TROPOMI-derived UT NO<sub>2</sub>

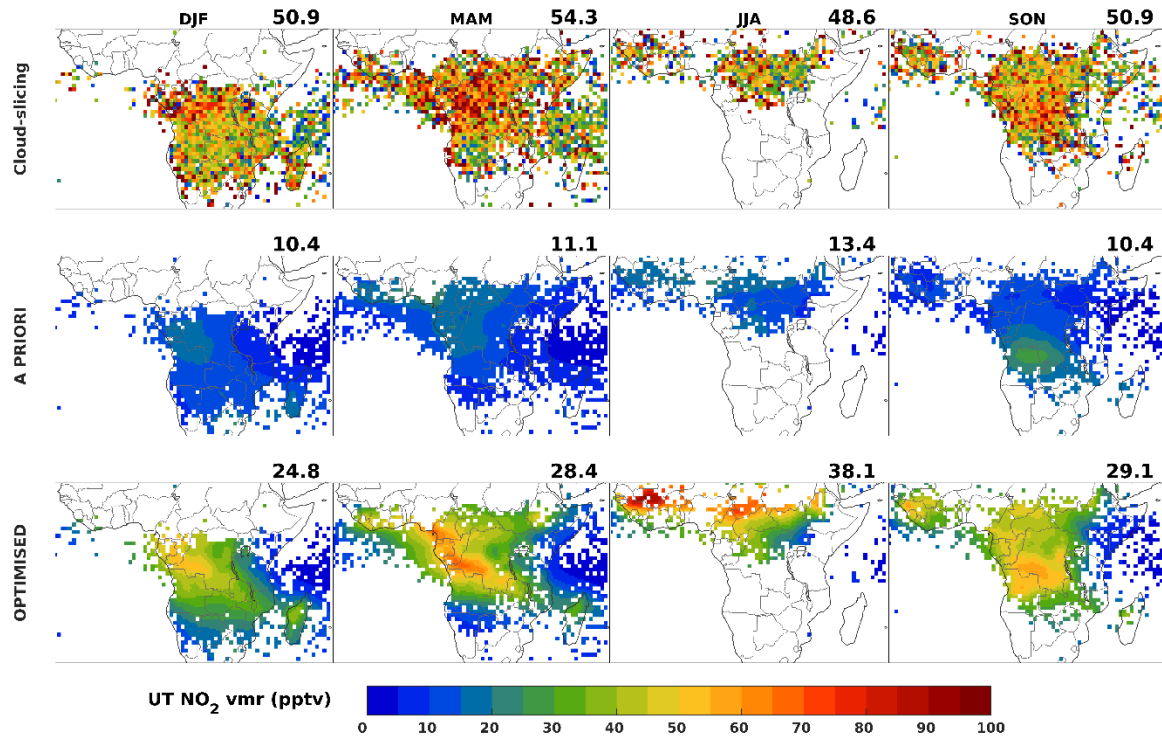


**Figure S3:** Seasonal distributions of upper-tropospheric NO<sub>2</sub> volume mixing ratios (in pptv) in December-January-February (DJF), March-April-May (MAM), June-July-August (JJA) and September-October-November (SON) from the cloud-sliced TROPOMI NO<sub>2</sub> over layer 320-180hPa of Horner et al. (2024) (top row), the *a priori* run (middle row) and the STD inversion (bottom row).

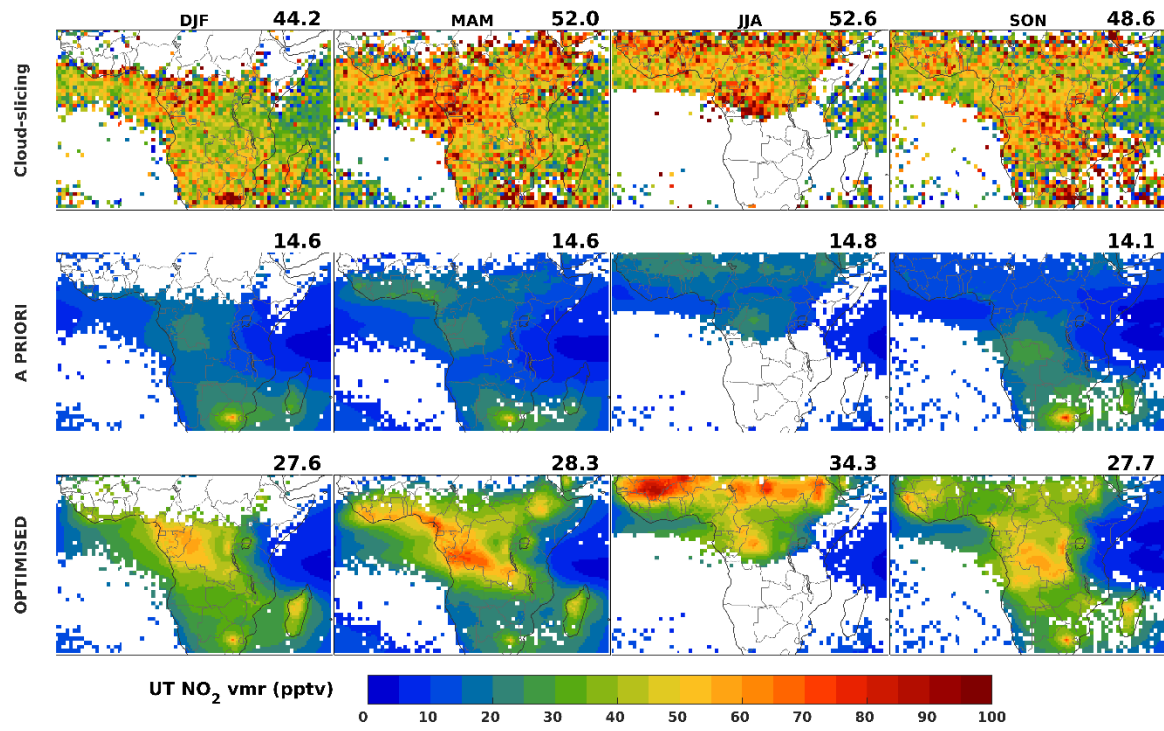
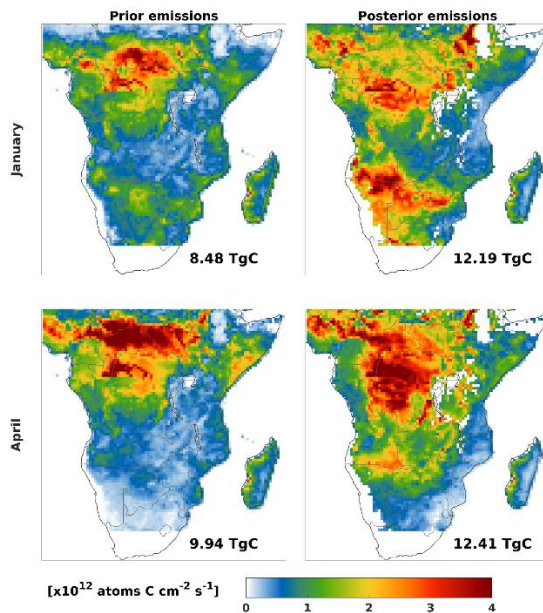


Figure S4: Same as in Fig. S3, but for layer 450-320hPa.

## 5. Optimised isoprene emissions

In order to compare our STD top-down isoprene fluxes based on TROPOMI HCHO and NO<sub>2</sub> with the CrIS-derived isoprene fluxes from Figure S13 of Wells et al. (2020), the following figure shows the *a priori* and top-down STD emissions for January and April 2019.



**Figure S5:** Spatial distribution of isoprene emissions (in  $10^{12}$  atoms C  $\text{cm}^{-2}$   $\text{s}^{-1}$ ) from the *a priori* (left column) and TROPOMI-based optimisation of isoprene emissions over the same region as in Wells et al. (2020) in January (top row) and April (bottom row). Total monthly emissions are provided inset (in TgC).